CHAPTER V

RESULTS AND DISCUSSION

5.1. Preparation and characterization of polymer-supported titanocene catalysts

The infrared spectroscopy is an effective method to follow each step in preparation of polymer-supported catalyst. It is sufficient to characterize the functional group in the wave number of 400-4000 cm^{-1}.

5.1.1. Preparation of polymer-supported catalyst using boron compound as cocatalyst

Preparation of polymer-supported catalyst using boron compound as cocatalyst shown in Figure 5.1.
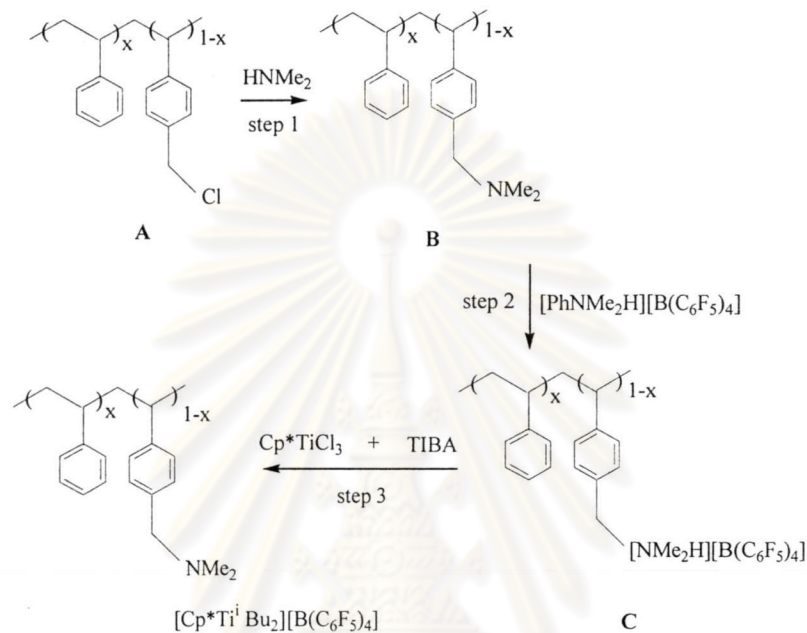
Figure 5.1. Preparation of polymer-supported catalyst using boron compound as cocatalyst.

Compound A: Polymer support: polystyrene-*co*-DVB

The absorption at 1265 cm^{-1} results from C-Cl bending vibration.

Compound B: PS-CH$_2$NMe$_2$

The absorption at 1255 cm^{-1} results from C-N bending and stretching vibrations from C-H absorption appear at 2765 and 2817 cm^{-1}.

Compound C: $PS-CH_2[NMe_2H][B(C_6F_5)_4]$

The absorption around 3303 cm^{-1} results from N-H stretching and absorption from perfluorophenylborate bending incorporation appear at 1644, 1516, 1086 and 973 cm^{-1}.

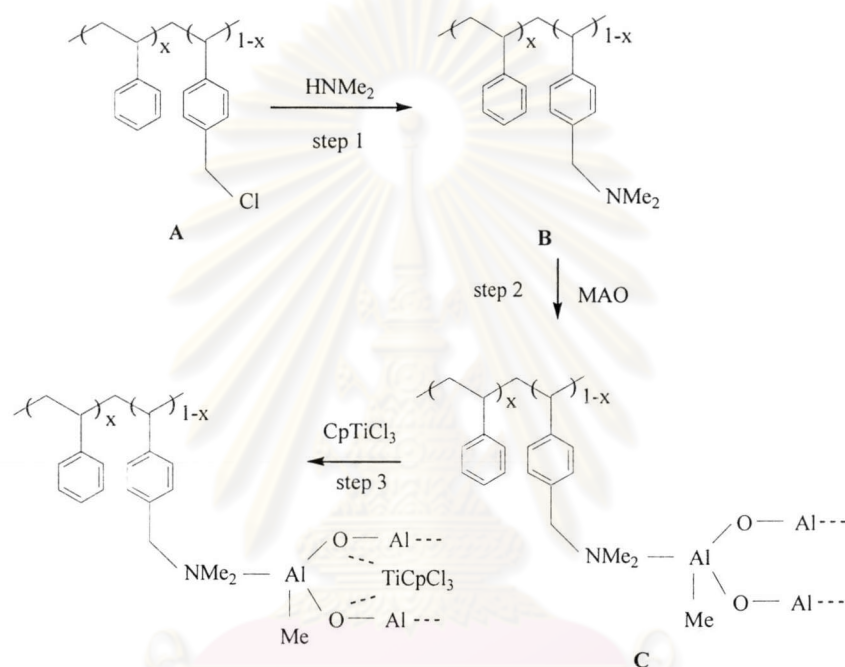The infrared spectra of compounds A, B and C are shown in Figure 5.2 [73].
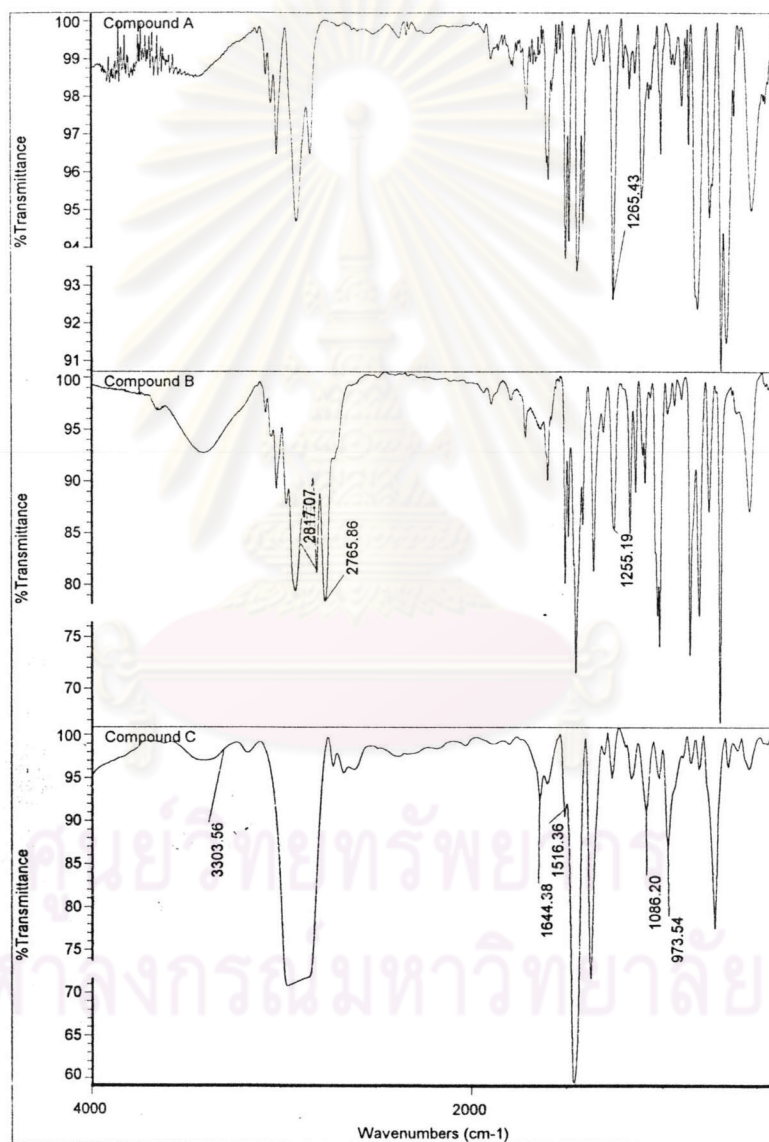
Figure 5.2. FTIR spectra of compounds A, B and C.

5.1.2. Preparation of polymer-supported catalyst using MAO as cocatalyst

Two methods for preparation of polymer-supported catalyst using MAO as cocatalyst were used.

Method A is shown in Figure 5.3.

Figure 5.3. Preparation of polymer-supported catalyst using MAO as cocatalyst (method A).

Compounds A and B are same as in Figure 5.1. The absorption of compound C at 726 cm^{-1} results from Al-N [71]. The infrared spectrum of compound C is shown in Figure 5.4.
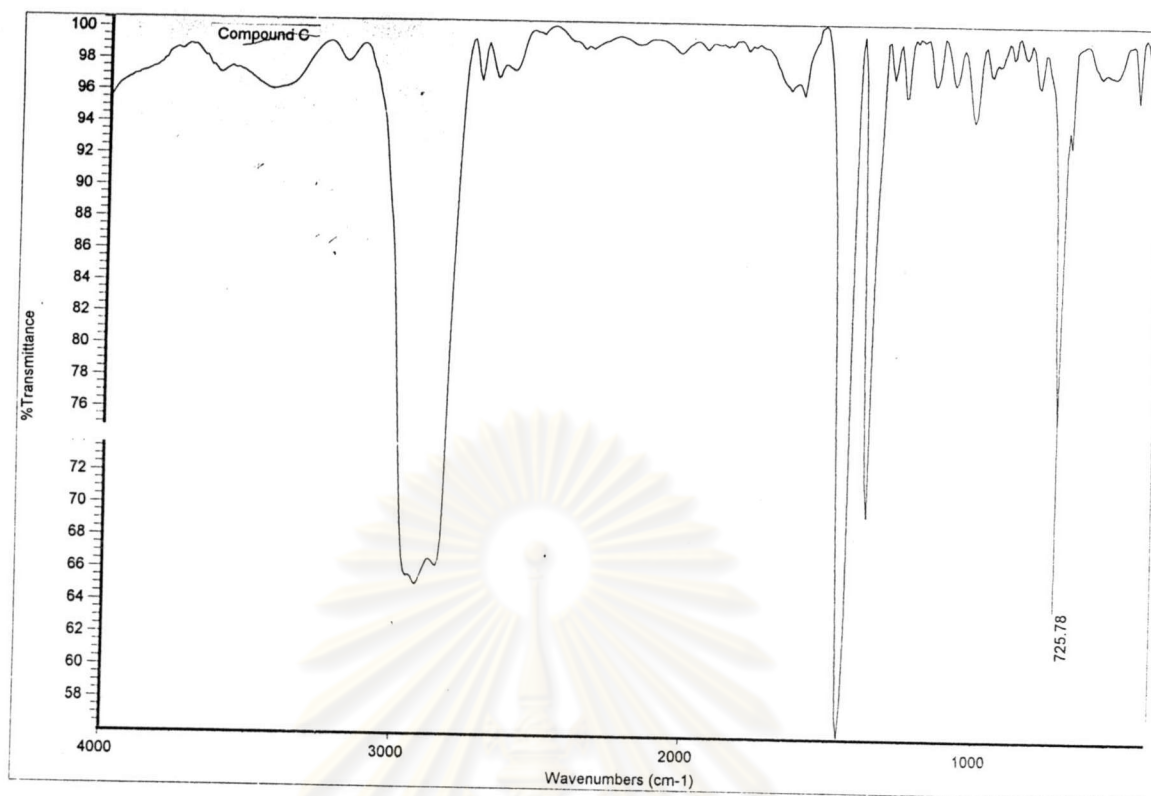
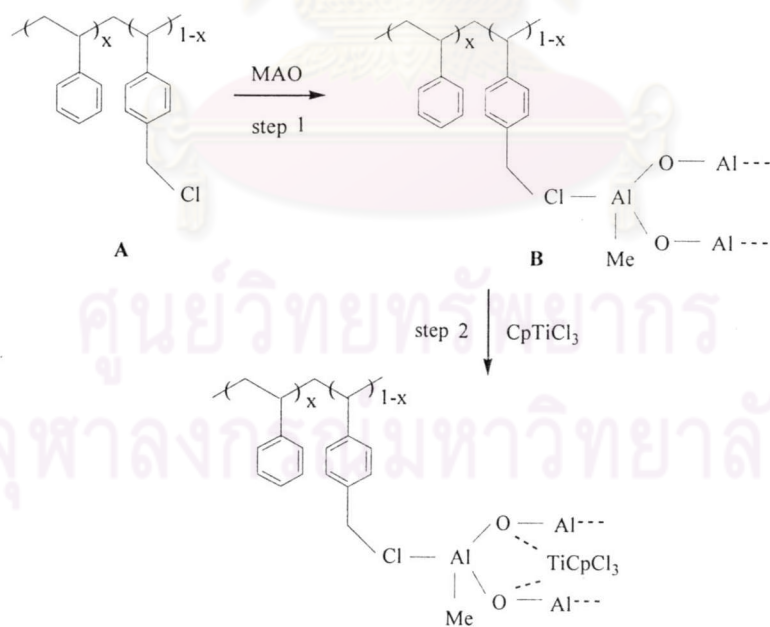**Figure 5.4.** FTIR spectrum of compound C.

Method B is shown in Figure 5.5.

Figure 5.5. Preparation of polymer-supported catalyst using MAO as cocatalyst (method B).

5.2. Homogeneous catalyst

5.2.1. CpTiCl₃/MAO system

The effects of Al/Ti molar ratio and polymerization temperature were investigated: molar ratio of Al/Ti 300 and 1000, polymerization temperature 30 and 50°C. The polymerization of styrene was performed for 4 h with 0.0100 mmol of catalyst. The results are shown in Table 5.1.

Table 5.1. Polymerization of styrene catalyzed by CpTiCl₃/MAO system

Al/Ti	T_P(°C)	Yield (g)	Activity($\times 10^{-3}$)	%SPS
300	50	0.53	192	76.5
1000	30	0.87	250	97.0

Activity = (kg of bulk polymer)/(mole of Ti • mole of styrene • h)

Styrene 10.00 mL (87.00 mmol)

From Table 5.1, the activity increases with increasing Al/Ti molar ratio. The role of MAO is to alkylate CpTiCl₃ catalyst and to generate active species, in addition, it acts as an impurity scavenger.

5.2.2. Cp*TiCl₃/TIBA/boron compound system

The three types of boron compound as cocatalyst were investigated; [PhNMe₂H] [B(C₆F₅)₄], [Ph₃C][B(C₆F₅)₄] and B(C₆F₅)₃. Styrene polymerization was conducted for 1 h at 70°C, at Al/Ti molar ratio of 200. The results are shown in Table 5.2.

Table 5.2. Polymerization of styrene catalyzed by Cp*TiCl₃/TIBA/boron compound system

[Ti] mmol	Cocatalyst	Yield(g)	Activity($\times 10^{-3}$)	%SPS
0.0050	[PhNMe₂H][B(C₆F₅)₄]	6.3500	14,597	92.1
0.0050	[Ph₃C][B(C₆F₅)₄]	7.3400	16,873	94.0
0.0050	B(C₆F₅)₃	0.2938	675	79.6

Activity = (kg of bulk polymer)/(mole of Ti • mole of styrene • h)

Styrene 10.00 mL (87.00 mmol)

From Table 5.2, three cocatalysts; [PhNMe₂H][B(C₆F₅)₄], [Ph₃C][B(C₆F₅)₄] and B(C₆F₅)₃ have efficiency in styrene polymerization. At 0.0050 mmol of catalyst, [Ph₃C][B(C₆F₅)₄] cocatalyst exhibits higher activity than the other two cocatalysts. Borate cocatalyst exhibits higher activity than borane cocatalyst. Ion pairing of borate cocatalyst as noncoordinating anion can be easily displaced by the olefin monomer [80].

5.3. Heterogeneous catalyst

5.3.1. Polymerization of styrene using boron compound as cocatalyst

The effects of amount of catalyst, polymerization temperature and molar ratio of Al/Ti were investigated: amount of titanium used for preparation of polymer-supported titanocene catalyst from 0.0050 to 0.1000 mmol, polymerization temperature 30°C and 70°C, molar ratio of Al/Ti 100 and 200. The experimental results are shown in Table 5.3.

Table 5.3. Polymerization of styrene by polymer-supported titanocene catalyst using various polymerization conditions

Entry	Catalyst	[Ti] mmol	Al/Ti molar ratio	Tp (°C)	Yield (g)	Activity ($\times 10^{-3}$)	%SPS
1	P-Cp*TiCl$_3$	0.0050	200	70	0.1000	17	96.8
2	P-Cp*TiCl$_3$	0.0100	200	70	0.1597	25	89.9
3	P-Cp*TiCl$_3$	0.0500	200	70	0.3558	16	83.2
4	P-Cp*TiCl$_3$	0.1000	200	70	0.5154	12	79.5
5	P-Cp*TiCl$_3$	0.0500	200	30	0.0805	0.6	91.3
6	P-Cp*TiCl$_3$	0.1000	100	70	0.1036	0.9	86.6
7	P-Cp*TiCl$_3$ after leaching	0.0500	200	70	0.3198	14	80.1
8	P-CpTiCl$_3$	0.0500	200	70	0.2331	9	79.1

Polymerization time (tp) 4 h and styrene 10.00 mL (87.00 mmol)

Activity = (kg of bulk polymer)/(mole of Ti • mole of styrene • h)

The results from entries 1-4 show that the optimum amount of catalyst is 0.0100 mmol. When the amount of catalyst is more than 0.0100 mmol, activity apparently decreases. The high activity at the low amount of catalyst could be attributed to the increasing of active species. The decreasing of activity with high amount of catalyst might be caused by the decline of active species due to dimerization of active species into inactive species [81].

The results from entries 3 and 5 show that activity increases with temperature. At low temperature, the π-olefin complex of titanium and styrene is more stable [82].

The results from entries 4 and 6 show that the activity is enhanced with increasing Al/Ti molar ratio. The function of TIBA is to alkylate the titanocene catalyst. The excess amount is needed because some is used to scavenge impurity in the system.

The results from entries 3 and 8 show that the activity of polymer-supported $Cp*TiCl_3$ is higher than that of polymer-supported $CpTiCl_3$ catalyst. The catalytic activity is enhanced by electron-releasing substituents on Cp* ligand. This result suggests stabilization of the active site by electron releasing substituents [60].

The results from entries 3 and 7 show that the activity of P-Cp*TiCl_3 before leaching and after leaching are comparable. This result confirms that titanocene does not drop into solution.

5.3.2. Polymerization of styrene using MAO as cocatalyst

There are two polymerization procedures for polymerization of styrene using MAO as cocatalyst.

Table 5.4. Two polymerization procedures

Procedure	
1	2
Polymer-supported titanocene catalyst/MAO system	Polymer-supported titanocene catalyst system
1. P-titanocene catalyst	1. P-titanocene catalyst
2. Styrene	2. Styrene
3. MAO	

In both procedures 10 mL of styrene (87 mmol) and P-titanocene catalyst were used. For procedure 1, additional MAO (3 mmol, 0.66 mL) was added in the system.

5.3.2.1. Polymer-supported titanocene catalyst (method A)

The effects of amount of catalyst and polymerization temperature were investigated: amount of titanium for preparation of polymer-supported titanocene catalyst

from 0.0100 to 0.1000 mmol and polymerization temperature 30°C and 70°C. The experimental results are shown in Table 5.5.

Table 5.5. Polymerization of styrene by polymer-supported titanocene catalyst (method A)

Entry	Catalyst	[Ti] mmol	Al/Ti molar ratio	Tp (°C)	Yield (g)	Activity (×10⁻³)	%SPS
9	P-CpTiCl₃/MAO	0.0100	300	50	0.1221	6	98.6
10	P-CpTiCl₃/MAO	0.0500	300	50	0.1751	4	96.3
11	P-CpTiCl₃/MAO	0.1000	300	50	1.0901	28	94.5
12	P-CpTiCl₃/MAO	0.1000	300	70	1.4756	39	96.7
13	P-CpTiCl₃	0.1000	300	50	0.1168	0.4	98.3
14	P-Cp*TiCl₃/MAO	0.1000	300	70	7.6805	217	98.5

Polymerization time (tp) 4 h and styrene 10.00 mL (87.00 mmol)

Activity = (kg of bulk polymer)/(mole of Ti • mole of styrene • h)

The results from entries 9-11 show that the catalytic activity increase markedly with increasing amount of catalyst.

The results from entries 11 and 12 show that higher temperature results in higher activity of catalyst.

The results from entries 11 and 13 show that polymer-supported CpTiCl₃ catalyst/MAO system exhibits a higher catalytic activity than polymer-supported CpTiCl₃ system. It can be concluded that MAO added to the system can enhance the catalytic activity, probably in impurity scavenge.

The results from entries 12 and 14 show that polymer-supported Cp*TiCl₃ catalyst system exhibits a higher catalytic activity than polymer-supported CpTiCl₃ catalyst system. This can be explained as that in the homogeneous catalytic system.

5.3.2.2. Comparison of polymer-supported CpTiCl₃ catalyst (method A) and polymer-supported CpTiCl₃ catalyst (method B)

Procedure 1 in 5.3.2 was used for polymerization of styrene, compared between supported catalyst prepared by methods A and B. The experimental results are shown in Table 5.6.

Table 5.6. Comparison between polymer-supported CpTiCl₃ catalysts prepared by (method A) and (method B)

Entry	Catalyst	[Ti] mmol	Al/Ti molar ratio	Tp (°C)	Yield (g)	Activity ($\times 10^{-3}$)	%SPS
12	P-CpTiCl₃/MAO (method A)	0.1000	300	70	1.4756	39	96.7
15	P-CpTiCl₃/MAO (method B)	0.1000	300	70	3.9531	110	97.4

Polymerization time (tp) 4 h and styrene 10.00 mL (87.00 mmol)

Activity = (kg of bulk polymer)/(mole of Ti • mole of styrene • h)

From Table 5.6 show that the catalyst prepared by method B exhibits a higher catalytic activity than method A. This can be explained that the coordinaiton of Cl-Al in method B is stronger than the coordination of N-Al in method A.

$\left(\underset{\text{Ph}}{}\right)_x \left(\right)_{1-x}$ ... Method A structure with:

Me—N—Me group, Al, Me, O—Al, TiCpCl$_3$, O—Al

$\left(\underset{\text{Ph}}{}\right)_x \left(\right)_{1-x}$ ... Method B structure with:

Cl—Al, Me, O—Al, TiCpCl$_3$, O—Al

Method A   Method B
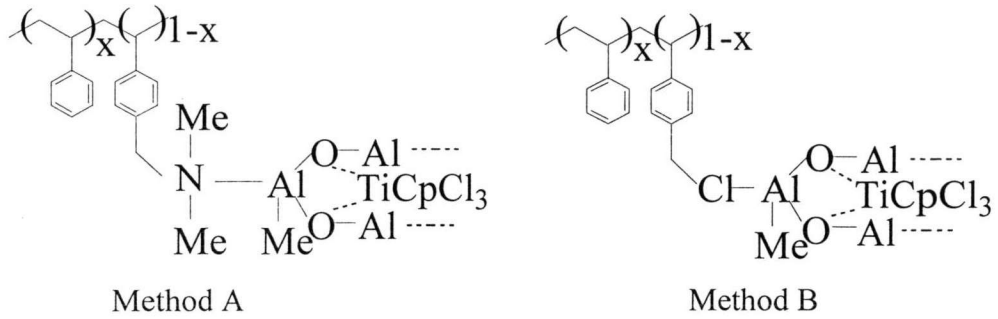
5.4.   Characterization of polystyrene

5.4.1. Nuclear magnetic resonance spectroscopy (NMR)

The tacticity of polymer is determined by ^{13}C NMR spectroscopy. Tacticity in NMR is represented by the relative configuration of pairwise units. A typical ^{13}C NMR spectrum of an atactic polymer in solution consists of numerous relatively sharp lines, that are assigned to the various sequences of meso (m) and racemic (r) dyads.

r   r   r   r   m   m   m   m

syndiotactic   isotactic
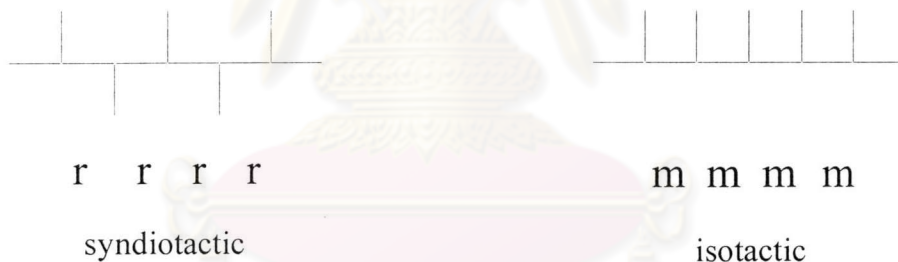
The ^{13}C NMR spectra of obtained polystyrene by P-CpTiCl$_3$ and P-Cp*TiCl$_3$ using MAO as cocatalyst are presented in Figures 5.6-5.7. The phenyl C$_1$ carbons resonate at 145 ppm, while the remaining aromatic carbon resonances appear at 128-133 ppm. The methine carbons are observed to resonate at 43 ppm. The methylene carbons exhibit sharp singlet at 41 ppm. Figure 5.8 shows ^{13}C NMR spectrum of the phenyl C$_1$ carbon of the three types of polystyrene [83], the spectrum of atactic polystyrene (Figure 5.8-(1)) shows five peaks in the range 145-146 ppm, corresponding to its various configurational sequences. The spectrum of isotactic polystyrene (Figure 5.8-(2)) shows the phenyl C$_1$ carbon as a single sharp peak at lower magnetic field ($\delta = 146$) corresponding to the mmmm pentad configuration. In contrast, a peak in syndiotactic

polystyrene (Figure 5.8-(3)) was observed at higher magnetic field (δ = 145). The obtained ^{13}C NMR spectrum corresponds with the result reported for SPS. Therefore, it is concluded that the produced polymer is syndiotactic polystyrene.
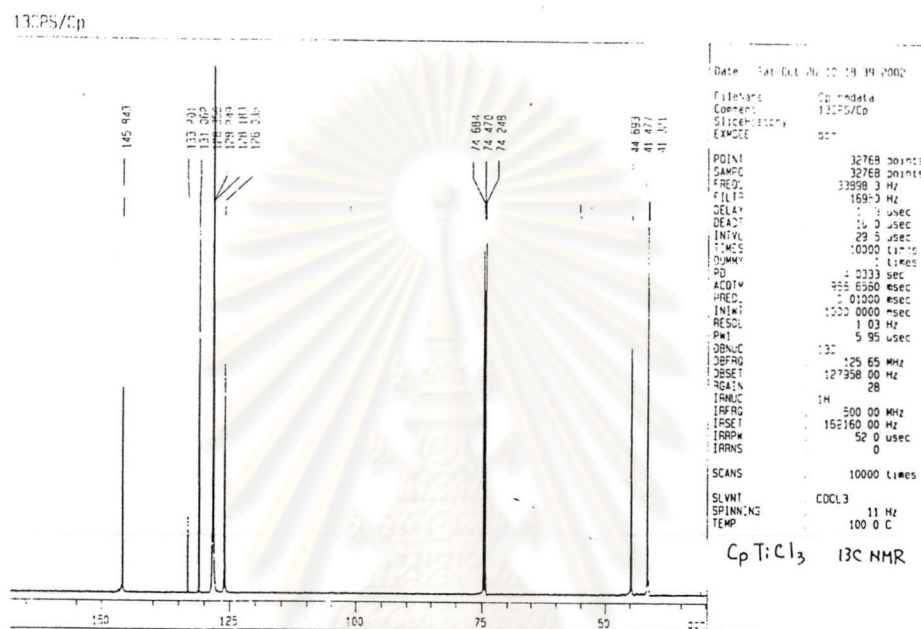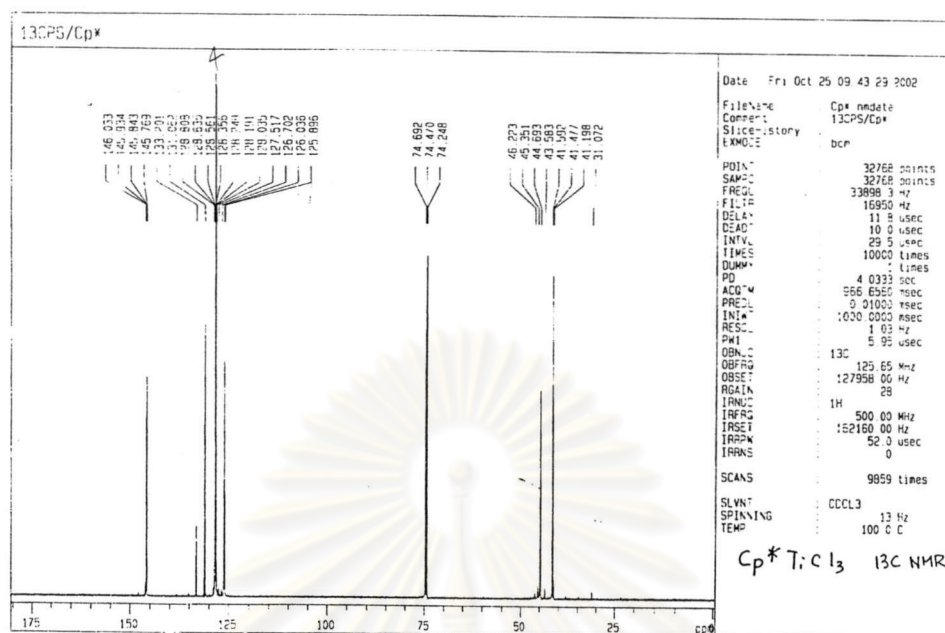

Figure 5.6. ^{13}C NMR spectrum of polystyrene obtained with P-CpTiCl$_3$ using MAO as cocatalyst.

Figure 5.7. ^{13}C NMR spectrum of polystyrene obtained with P-Cp*TiCl$_3$ using MAO as cocatalyst.
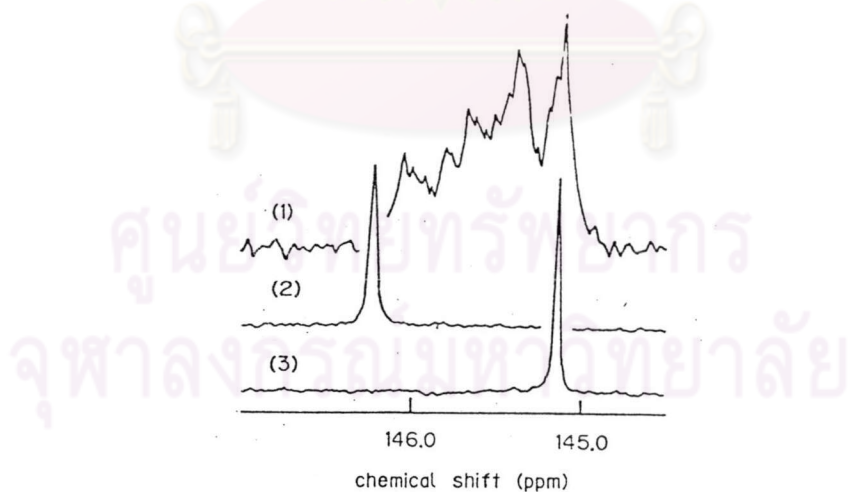
Figure 5.8. ^{13}C NMR spectra of polystyrene: (1) atactic; (2) isotactic; (3) syndiotactic.

5.4.2. Scanning electron microscopy (SEM)

The morphological properties of polystyrene-*co*-DVB bead and polystyrene products obtained by different catalytic systems were shown in Figures 5.9-5.12.

Figure 5.9 shows the SEM micrograph of a smooth surface of polystyrene-*co*-DVB bead. Figure 5.10 shows the SEM micrograph of homogeneous Cp*TiCl$_3$/TIBA/boron compound. Figures 5.11-5.12 show SEM micrographs of polystyrene product by polymer-supported catalyst using boron compound and polymer-supported catalyst using MAO as cocatalyst, respectively. The morphology of polystyrene synthesized from polymer-supported catalysts is spherical. The shape of polymer particles is a replica of that of the carrier particle.
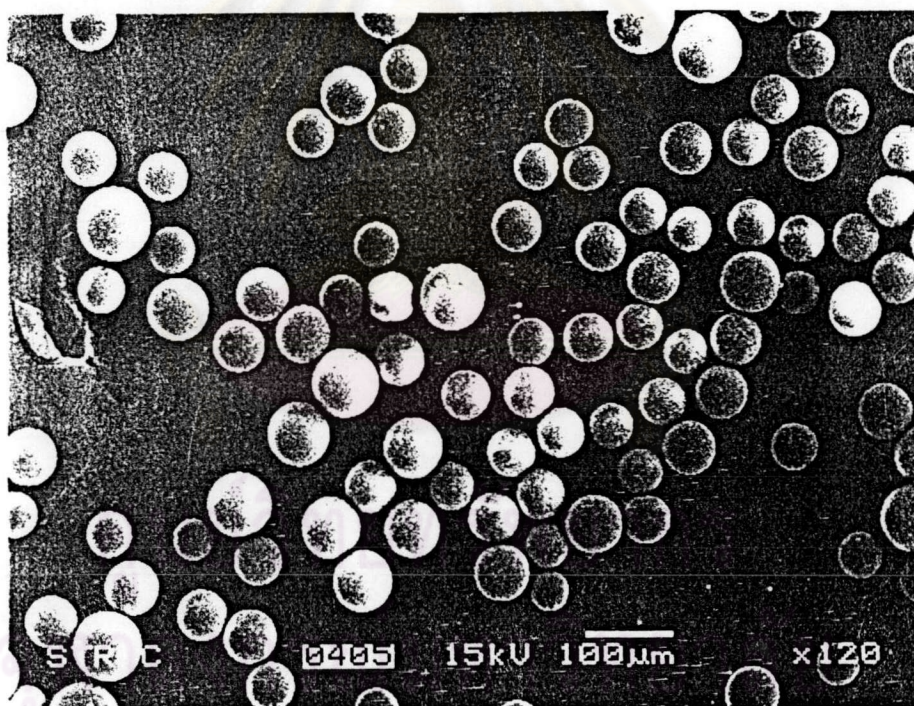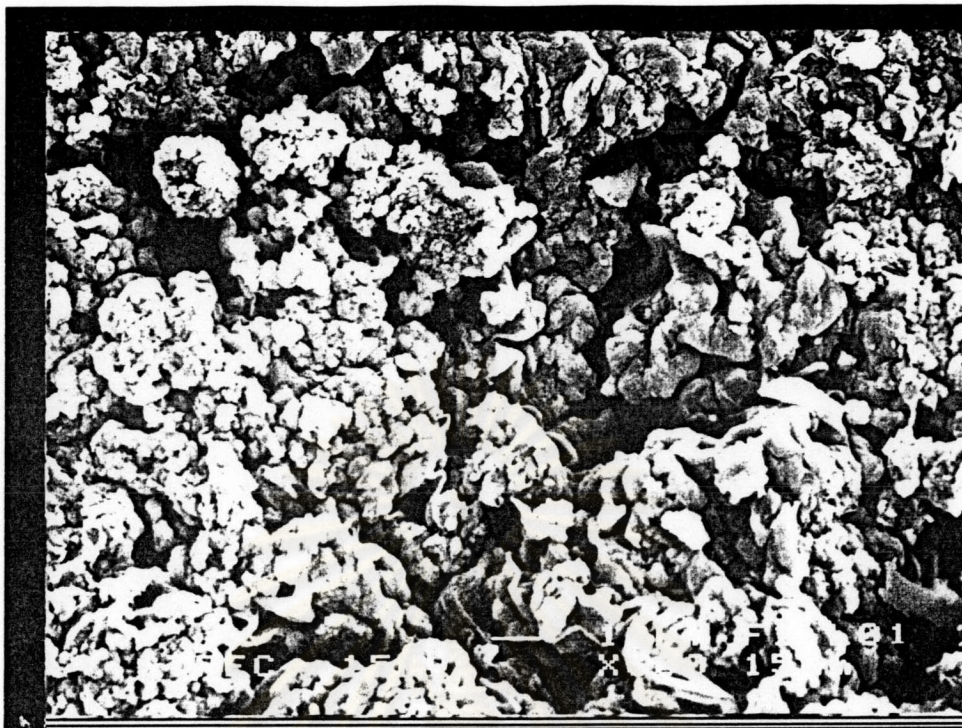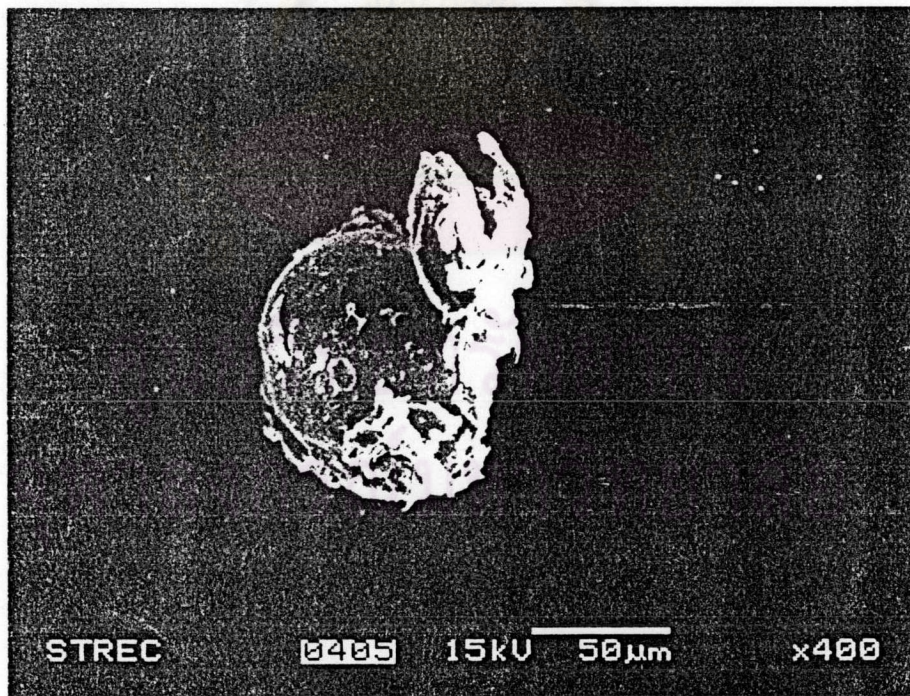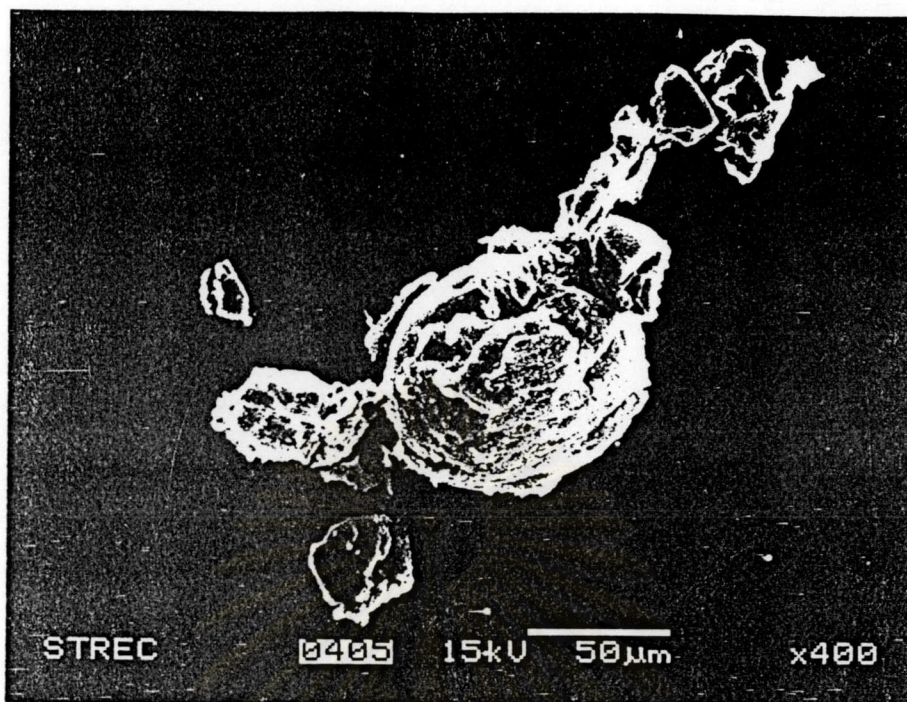

Figure 5.9. SEM micrograph of polystyrene-*co*-DVB bead.

Figure 5.10. SEM micrograph of polystyrene produced with homogeneous Cp*TiCl$_3$/TIBA/boron compound.

Figure 5.11. SEM micrograph of polystyrene produced with polymer-supported catalyst using boron compound as cocatalyst.

Figure 5.12. SEM micrograph of polystyrene produced with polymer-supported catalyst using MAO as cocatalyst.

5.4.3. Molecular weight (M_w) and molecular weight distribution (MWD)

The molecular weight and molecular weight distribution of polystyrene produced by P-CpTiCl$_3$/MAO and P-Cp*TiCl$_3$/MAO systems are presented in Table 5.7. The GPC curves are shown in Figures 5.13-5.14.

Table 5.7. M_w and MWD of the obtained polystyrene by P-Cp*TiCl$_3$/MAO and P-CpTiCl$_3$/MAO systems

Catalyst system	M_W	M_n	M_W/M_n
P-Cp*TiCl$_3$/MAO	40,304	17,098	2.3
P-CpTiCl$_3$/MAO	190,349	52,564	3.6

From Table 5.7, molecular weight (M_W) and molecular weight distribution (M_W/M_n) of polystyrene produced with P-Cp*TiCl$_3$/MAO system are 40,304 and 2.3 respectively. For P-CpTiCl$_3$/MAO system molecular weight (M_W) and molecular weight distribution of polystyrene produced are 190,349 and 3.6 respectively. The polymer supported system (PSOH/CpTiCl$_3$-MAO system) was reported to have molecular weight (M_W) and molecular weight distribution of 44,500 and 2.2 respectively [67]. Therefore it seems that the polymerization condition affect on the Mw.

	分子量分布名	Mn	Mw	MP	Mz	Mz+1	Mv	分散度
1	PS-Cp	52564	190349	209333	331375	513689	175073	3.621
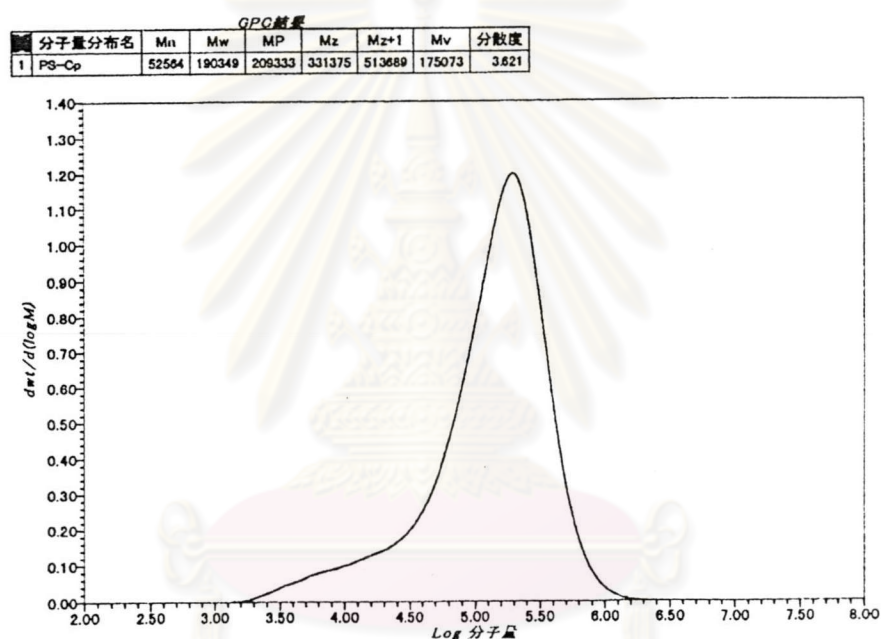
Figure 5.13. GPC curve of polystyrene produced with polystyrene obtained with P-CpTiCl$_3$ using MAO as cocatalyst.

	分子量分布名	Mn	Mw	MP	Mz	Mz+1	Mv	分散度
1	PSCps	17098	40304	32846	77035	120855	38744	2.357
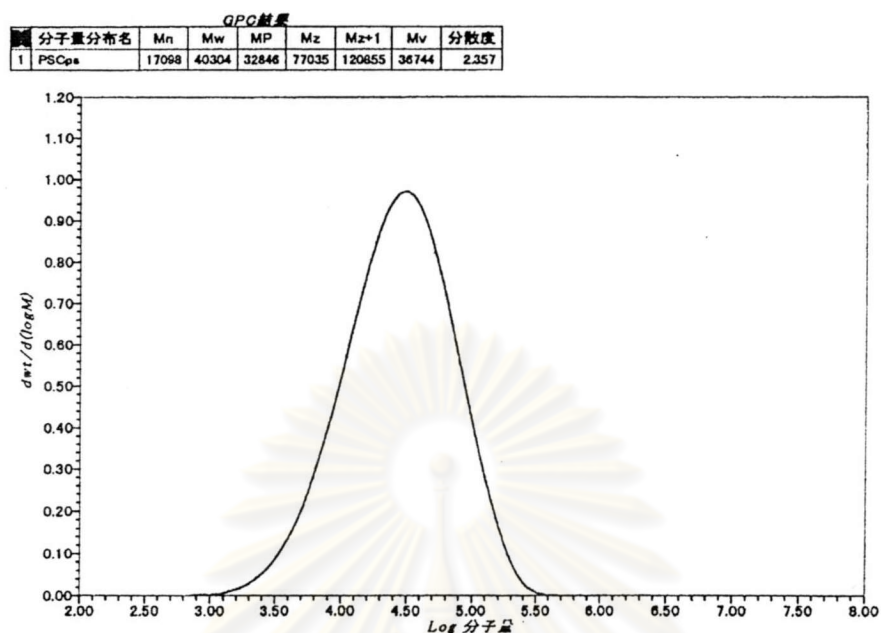
Figure 5.14. GPC curve of polystyrene produced with polystyrene obtained with P-Cp*TiCl$_3$ using MAO as cocatalyst.

5.4.4. Melting temperature (T$_m$)

The melting temperature of polystyrene produced by Cp*TiCl$_3$/boron, P-Cp*TiCl$_3$-boron and P-Cp*TiCl$_3$-MAO system are presented in Table 5.8. The DSC curves are shown in Figures 5.15-5.16.

Table 5.8. T$_m$ of the obtained polystyrene by Cp*TiCl$_3$/boron, P-Cp*TiCl$_3$-boron and P-Cp*TiCl$_3$-MAO system

Catalyst system	T$_m$ (°C)
Cp*TiCl$_3$/boron	270.8
P-Cp*TiCl$_3$-boron	250.1
P-Cp*TiCl$_3$-MAO	270.6

From Table 5.8, melting temperature (T_m) of polystyrene produced with Cp*TiCl$_3$/boron, P-Cp*TiCl$_3$-boron and P-Cp*TiCl$_3$-MAO is 270.8, 250.1 and 270.6 respectively. It can be confirmed that the polystyrene product is syndiotactic polystyrene [67].
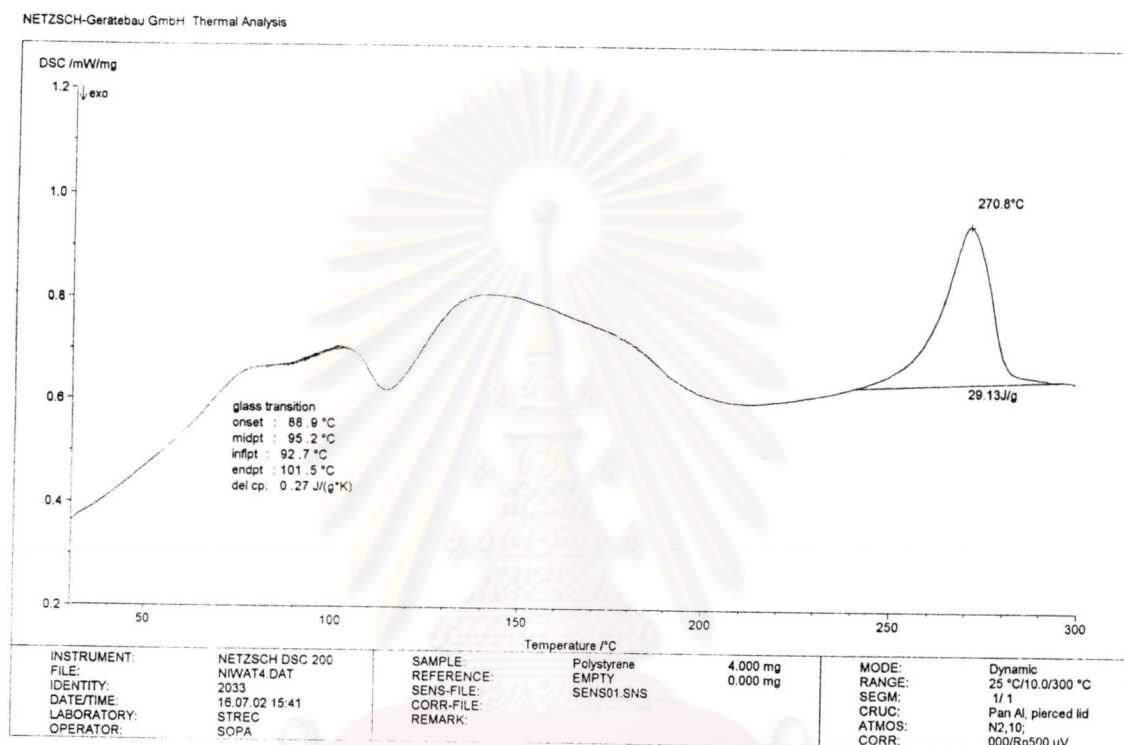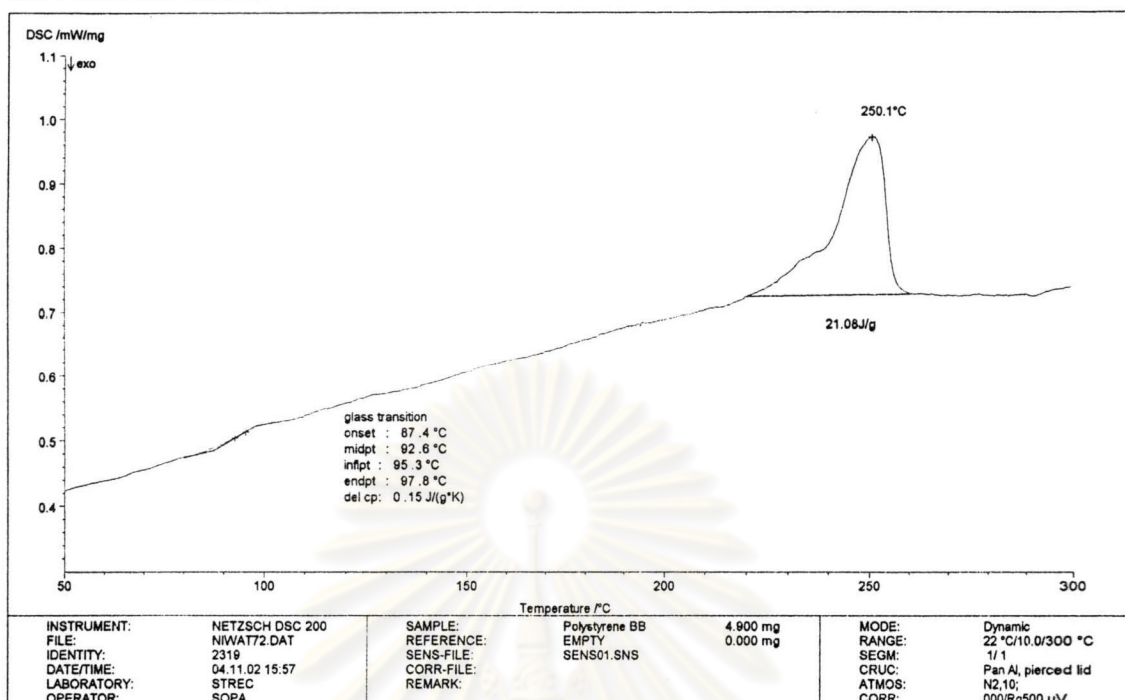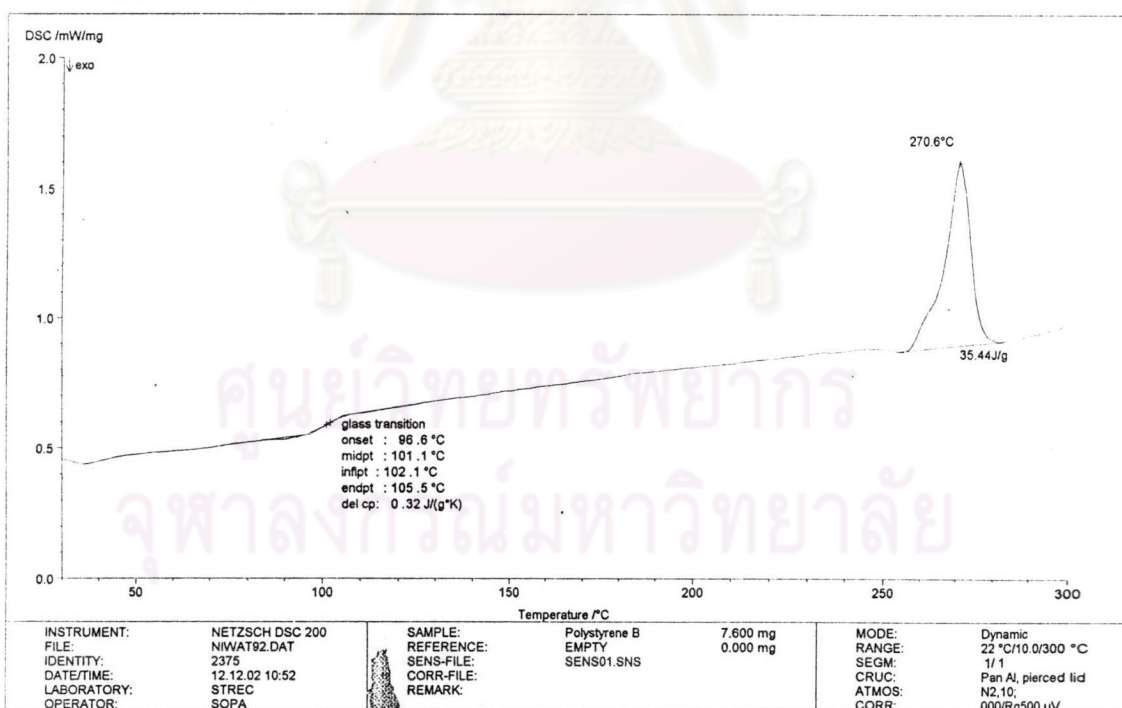

Figure 5.15. DSC curve of polystyrene produced with Cp*TiCl$_3$/boron system.

Figure 5.16. DSC curve of polystyrene produced with P-Cp*TiCl₃-boron system.

Figure 5.17. DSC curve of polystyrene produced with P-Cp*TiCl₃-MAO system.